

SUPPLEMENTARY METHODS

Assumptions of the model. DNA replication in an *S. pombe* cell was modeled as a two-step process. In step 1 pre-RCs were assembled at a fixed number of sites in the genome. The positions of the pre-RCs were chosen at random according to a probability distribution describing the relative likelihood of a pre-RC at each position in the genome. In step 2 assembled pre-RCs were fired, and new DNA strands synthesized. It was assumed that all assembled pre-RCs are equivalent; they fire at random at an instantaneous rate (probability per unit time) that increases during S phase. Consistent with previous data (1) it was assumed that the firing rate increases linearly with time during S phase until it reaches a maximum rate. Finally, it was assumed that the velocity of the replication forks established at each fired pre-RC is constant and that replication forks cause disassembly of unfired pre-RCs that they encounter.

Parameters. The model has a maximum of six parameters as follows: the number of pre-RCs per cell, the rate of increase in the probability of pre-RC firing per unit time, the maximum pre-RC firing rate, the fork velocity, the transcription indicator variable, and the exponential rate constant relating the probability of pre-RC assembly to local AT content (see below).

Implementation of the model. The model with the assumptions described above was implemented in the Java programming language. For a given set of replication parameters, we simulated the replication of 1000-2000 chromosomes.

Probability distributions. As described in the text, we implemented two probability distributions for positioning pre-RCs. To simulate the outcomes of DNA combing experiments, which provide information about the number and spacing of initiation events at various times during S phase, but no information about the local fluctuations in the probability of initiation, pre-RC sites were chosen from a uniform probability distribution. This procedure generated an exponential distribution of distances between initiation sites as observed in DNA combing experiments (2). To simulate the outcomes of Pu-seq experiments, which provide high resolution information about local fluctuations in the frequency of initiation along the genome,

pre-RC sites were chosen from a probability distribution that incorporated the influences of the high affinity of ORC for AT tracts and the interference of transcription with stable pre-RC formation. For this distribution, the relative probability of pre-RC assembly at position x was given by $\text{Pr}(x) \propto T(x) \times e^{[C \times AT(x)]}$, where $AT(x)$ is the AT content of a 25 bp window with x at its center, C is a constant, and $T(x)$ has value 0 if the window overlaps a transcription unit and value 1 otherwise. For each molecule whose replication was simulated, pre-RC sites were sequentially chosen according to the distribution $\text{Pr}(x)$. Pre-RC sites within 25 nucleotides of a previously chosen site were disallowed to account for possible steric exclusion. The positions of transcription units were obtained from a Genbank annotation of *S. pombe* chromosome 2 (Schizosaccharomyces_pombe.ASM294v2.23). Blocks of transcribed DNA included annotated mRNAs, tRNAs, snoRNAs, snRNAs, and rRNAs. Non-coding RNAs were not included because of many uncertainties about their levels of expression.

States of pre-RC sites. During simulation of replication of a molecule, a linked list of pre-RC sites was continuously updated to maintain the following state information: the current status of the pre-RC site (potential, activated, completed or disassembled), and the current status of the two replication forks that originated at each pre-RC (fork active or inactive and fork position).

DNA synthesis. Simulation of DNA synthesis was carried out in intervals of 0.01 min. For each interval, the probability of initiation per pre-RC and the nominal number of nucleotides added at each fork were calculated. Pre-RC sites were then scanned twice, first, to trigger possible changes of state due to initiation events (potential pre-RC to active pre-RC) and second, to increment fork positions and trigger changes in state due to the merger of forks (fork termination) or disassembly of pre-RCs by forks. When both forks originating at a given pre-RC site terminated synthesis the state of the pre-RC changed from active to completed. When a fork passed a site with an inactive pre-RC, the state of the latter changed from potential to disassembled. Intermediate states of replicating molecules were recorded at regular intervals or when the percent replication reached that of a combed DNA molecules in the dataset of Kaykov and Nurse (1).

Population averages. The values of a number of replication variables were averaged over a population of 1000-2000 molecules replicated with a specified set of parameters. Population averages included the number of initiations, the number of replication forks, the number of closures (events in which two converging forks meet), and the percent replication as functions of time in S phase. The average fraction of rightward (or leftward) moving forks and the median time of replication were calculated as functions of position in the chromosome.

Optimization procedure. The DNA combing data of Kaykov and Nurse (1) were used to optimize the following three parameters: the number of pre-RCs, the rate of increase of the pre-RC firing probability per unit time and the maximum rate of pre-RC firing. In most simulations a fork velocity of 2 kb per min was assumed, although the effect of changing this value was also explored (see text for details). The replication parameters were systematically varied and their optimal values were determined by selecting those that minimized the mean squared deviation (MSD) between the number of forks per Mb observed in combed DNA molecules in the Kaykov and Nurse (1) dataset and the number of forks per Mb predicted by the simulation. The rate of increase in the probability of pre-RC firing per unit time at the minimum MSD was 0.022 events/pre-RC/per min². This value corresponds to a firing rate of 0.175 initiations/min per pre-RC at 8 min, the time of maximal DNA synthesis in the simulations. The optimized maximum firing rate of 0.3 initiations/min per pre-RC was not reached until 13-14 min at which time nearly all pre-RCs had either fired or been disassembled by forks, so setting the maximum rate at higher values had little or no effect. Thus, the rate of firing of pre-RCs increased continuously during the period that the vast majority of initiations occurred. As described in the text, the DNA combing data did not constrain the density of pre-RCs at the upper bound. The MSD declined until the number of pre-RCs per Mb reached 80 per Mb but remained constant at higher pre-RC densities.

The polymerase usage data were used to optimize the constant C in the function $Pr(x)$ describing the probability of pre-RC assembly at each position in the genome (see above). This constant is the factor that relates the probability of pre-RC assembly to local AT content at positions outside transcription units. The value of C was systematically varied in

simulations performed with the optimized values of the firing parameters derived from the DNA combing experiments as described above. A value of $C = 21$ was obtained at the minimum MSD between the observed rightward fork frequencies across chromosome 2 and those predicted by the simulation.

Cytometry of cells pulse labeled with EdU. Cells of *S. pombe* strain FY2317 growing logarithmically in YE6s rich medium (3) were pulse-labeled for 10 min with 200 μ M EdU and fixed in 70% EtOH. The cells were washed with 1 mL TE (10mM Tris , 1mM EDTA, pH 8), resuspended in 200 μ L TE + 2 μ L 10 mg/mL RNaseA and incubated at 37 $^{\circ}$ C for 2 h. After resuspension in 200 μ L of Alexa Fluor 647 click reaction mix (Life Technologies C10640), the cells were incubated 30 min at RT in the dark. Samples were chilled on ice for 5 min, washed twice with 1 mL PBS, resuspended in 10 μ L PBS. An aliquot of the cell suspension (5 μ L) was dried on the surface of a 4 mL agarose pad cast in a 35 mM glass-bottomed petri dish (2% agarose LE in TE, plus 5 μ g/mL sytox green). The pad was then re-inserted into the petri dish and cells were imaged with a Leica SP8 confocal microscope using a 63X glycerol objective. Between 9 and 13 Z sections spanning the cells were obtained at 1 μ M intervals.

Images of the cells were processed and quantified using FIJI. Well-focused Z sections were selected and projected into a single image by taking the sum. Cell length was measured manually using a well-focused DIC image. The cell periphery was defined using the magic wand tool on the red image (EdU labeled with Alexa Fluor 647). The nuclear periphery was defined using the magic wand tool on the green image (Sytox green DNA stain). Red fluorescence was quantified for 395 mononucleate cells from a population of 500 cells.

SUPPLEMENTARY FIGURE LEGENDS

Figure S1. Optimization of the number of pre-RCs assembled in each cell. Simulations of the replication of chromosome 2 were performed with different numbers of pre-RCs per Mb ranging from 20 to 120. Pre-RC sites were chosen from a uniform probability distribution, which generated an exponential distribution of the distances between pre-RCs. The replication parameters were optimized for each number of pre-RCs as described in Supplementary

Methods. **A.** Root mean square deviation between the observed density of replication forks in 160 combed DNA molecules in the Kaykov and Nurse (1) dataset and the density of replication forks predicted by the simulations as a function of the number of pre-RCs per cell. As the density of pre-RCs was increased, the deviation decreased reaching a plateau at about 80 pre-RCs per Mb. The combing data do not constrain the maximum value of the number of pre-RCs because increases in the density of starting pre-RCs above 80 per Mb were compensated by decreases in the optimized rate of firing per pre-RC. **B.** The number of initiations and pre-RCs disassembled by passage of forks as a function of the number of pre-RCs. As the number of pre-RCs per cell was increased the predicted number of initiations approached a constant value and the predicted number of disassembled pre-RCs increased. Thus, the major effect of increasing the number of pre-RCs above 80 per MB is to reduce the overall efficiency of utilization of assembled pre-RCs.

Figure S2. Duration of S phase determined by pulse labeling with EdU. *S. pombe* cells enter S phase after the completion of M phase and a very short G1 phase. The duration of S phase has been estimated at 10% of the cell cycle or about 15 minutes (4). According to this estimate, S phase is largely completed by the time of cell division (16 min after the onset of S phase), so that newly born cells would be expected to be in G2 phase with a 2 C DNA content. Our model predicts a period of rapid DNA synthesis followed by a long period during which the rate of DNA synthesis is low and declining, suggesting that S phase may extend well into the period generally regarded as G2 phase. The model also predicts that the duration of S phase is heterogeneous in a cell population. To test these predictions, we quantified nascent DNA synthesis from cell birth to M phase by pulse labeling cells with the thymidine analog 5-ethynyl-2-deoxyuridine (EdU). After covalently coupling the analog to a fluorophore (5), the incorporation of EdU into DNA was quantified by confocal microscopy. The length of each cell was also measured to determine its age after birth. **A.** Nuclear EdU signal as a function of cell length. Cells were pulse labeled with EdU for 10 min and the incorporation into nuclear DNA was quantified in mononucleated cells. The cells were binned into length categories spanning 1 μ M. The average incorporation into cells of each category (with 95% confidence limits

indicated) was plotted against the length at the midpoint of each category. An EdU signal above background can be detected from the birth of the cells until the cells reach a length of at least 10 μM , which corresponds to about 39 minutes after cell birth (see panel E). Thus, taking into account the length of the pulse, the duration of S phase is at least 45 minutes (39 min post birth plus 16 min from onset to birth minus 10 min pulse length) in some cells in the population, confirming the prediction that S phase continues at a low and declining rate long after the burst of DNA synthesis prior to cell birth. It follows that DNA synthesis continues well into the period generally regarded as G2 phase. These results are similar to those of a prior experiment in which *S. pombe* DNA synthesis was quantified by autoradiographic grain counting (4). **B.** Cytoplasmic EdU Signal as a function of cell length. The cytoplasmic EdU signals are low compared to the nuclear signal and increase slightly with cell length. **C, D.** Scatter diagram and violin plot showing the distribution of EdU incorporation as a function of cell length. The cells (circles in the scatter plot) are binned in 1 μM length intervals. The numbers above the scatter plot indicate the fraction of cells with EdU incorporation above the background level of 0.6, which is the limit of sensitivity of the experiment. These values should be considered a lower bound on the fraction of cells that have not yet completed DNA replication because low levels of DNA synthesis may fall below this limit of sensitivity, i.e. some cells may not complete DNA replication until later in the cell cycle. As the cells progress through the cell cycle more and more of them complete DNA replication. Most of the cells have reached the background level of incorporation by the time that they reach a length of 10.5 μM corresponding to about 47 min after birth. The results clearly indicate that the duration of S phase is heterogeneous in the cell population as predicted by the model. The red line in the violin plot shows the median EdU incorporation as a function of cell length. **E.** The relationship between cell length and cell age. Cell length and the elapsed time from birth were determined using live-cell imaging as described previously (n = 600 cells) (6).

Figure S3. Time course of DNA replication. The replication of chromosome 2 was simulated using the following parameters: pre-RC density: 80 per Mb; rate of increase of firing probability per min: 0.022 events/ min^2 per pre-RC; maximum firing rate: 0.3 events/min per pre-RC; fork

velocity: 2 kb/min; exponential coefficient for AT content: 21. For each time point in S phase, the fraction of cells that had replicated each 300 bp segment is plotted against the position of the segment. The major peaks of nascent DNA synthesis (efficiencies greater than 15%) described in the origin mapping study of Heichinger, Penkett, Bahler and Nurse (7) are shown as red dots. The data of Heichinger, Penkett, Bahler and Nurse (7) were obtained from cells treated with hydroxyurea to limit fork movement, and DNA contents at various positions in the genome were assessed by hybridization to microarrays of DNA probes with an average inter-probe distance of 1.3 kb.

Figure S4. Frequency distribution of initiations and termination. The fraction of 300 bp segments of chromosome 2 with a given frequency of initiation (or termination) per cell was determined by averaging the results of simulating the replication of 10,000 molecules. Although the distribution is quite heterogeneous, the probability of initiation in the majority of 300 bp segments is below 0.15. The probability of termination has a more uniform distribution with a value in the neighborhood of 0.01 for most 300bp segments.

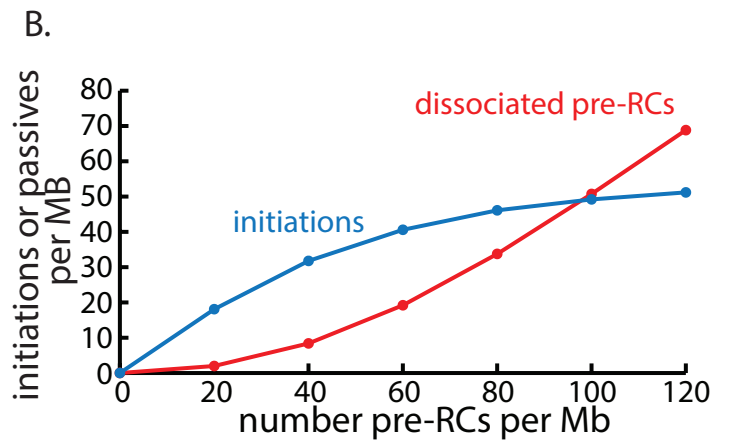
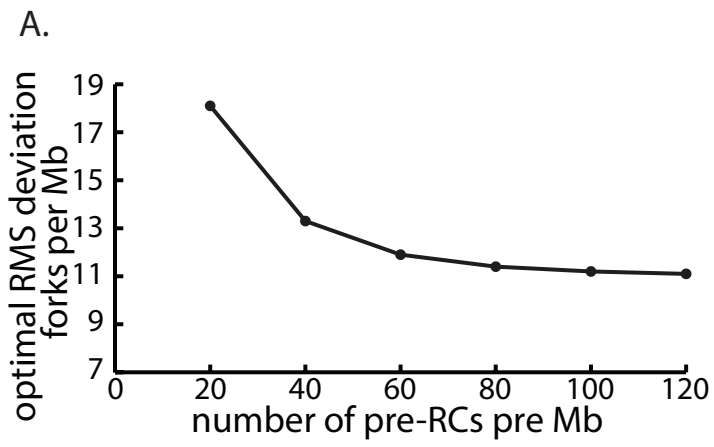
Figure S5. High resolution view of the probability of termination. The probability of termination in each 300 bp segment of a segment of chromosome 2 from figure S4 is plotted at larger scale. The rightward fork frequency of the same segment is plotted below the termination frequency.

Figure S6. Correlation of median replication time with size of transcript. The average median time of replication of the centers of transcription units predicted by simulation is plotted as a function of the size of the unit. Because of exclusion of initiation events from transcription units, the time of replication of the centers of such units increases with their size.

REFERENCES

1. Kaykov A & Nurse P (2015) The spatial and temporal organization of origin firing during the S-phase of fission yeast. *Genome Res* 25(3):391-401.
2. Patel PK, Arcangioli B, Baker SP, Bensimon A, & Rhind N (2006) DNA replication origins fire stochastically in fission yeast. *Mol Biol Cell* 17(1):308-316.
3. Hodson JA, Bailis JM, & Forsburg SL (2003) Efficient labeling of fission yeast *Schizosaccharomyces pombe* with thymidine and BUdR. *Nucleic Acids Res* 31(21):e134.
4. Nasmyth K, Nurse P, & Fraser RS (1979) The effect of cell mass on the cell cycle timing and duration of S-phase in fission yeast. *J Cell Sci* 39(215):215-233.
5. Sabatinos SA, Green MD, & Forsburg SL (2012) Continued DNA synthesis in replication checkpoint mutants leads to fork collapse. *Mol Cell Biol* 32(24):4986-4997.
6. Callegari AJ & Kelly TJ (2006) UV irradiation induces a postreplication DNA damage checkpoint. *Proc Natl Acad Sci U S A* 103(43):15877-15882.
7. Heichinger C, Penkett CJ, Bahler J, & Nurse P (2006) Genome-wide characterization of fission yeast DNA replication origins. *Embo J* 25(21):5171-5179.

Figure S1



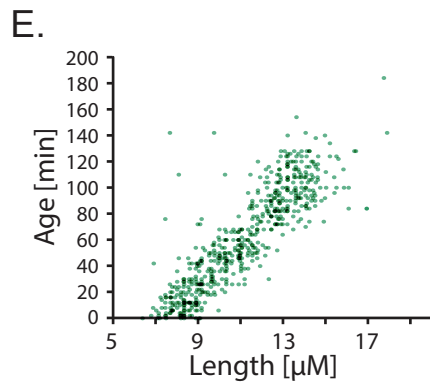
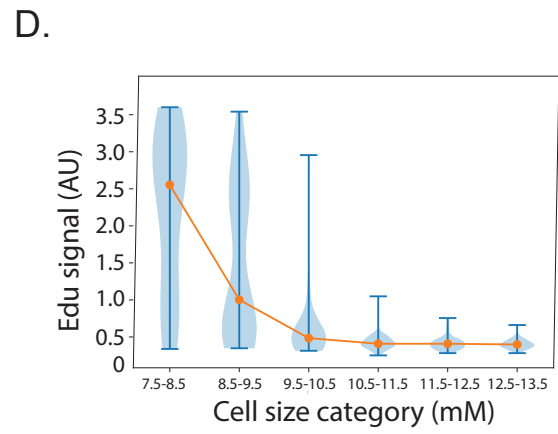
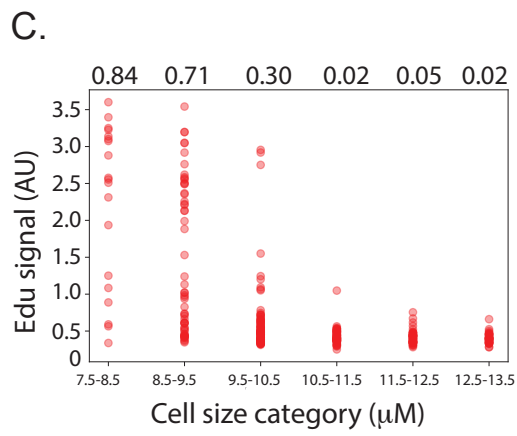
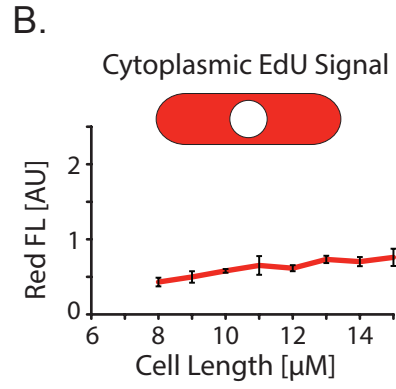
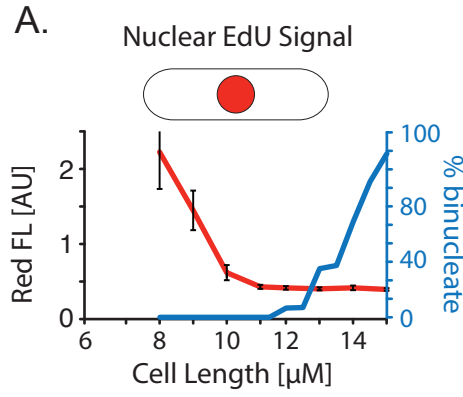


Figure S3

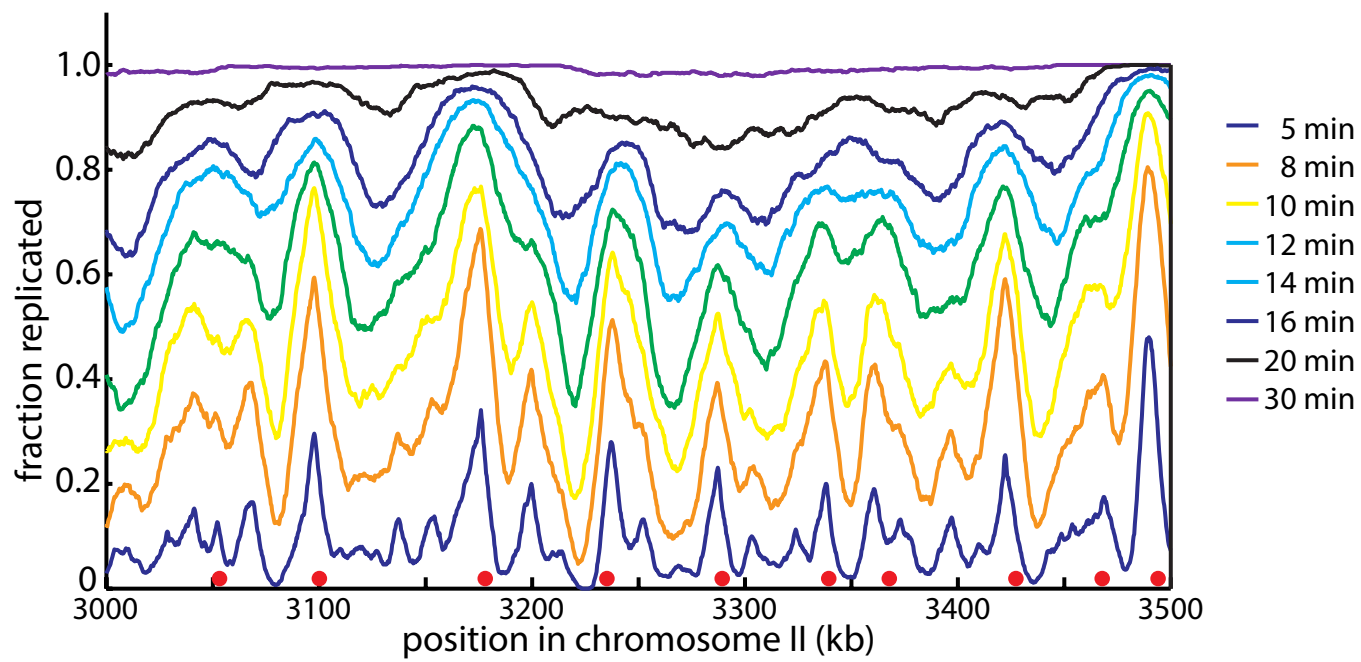


Figure S4

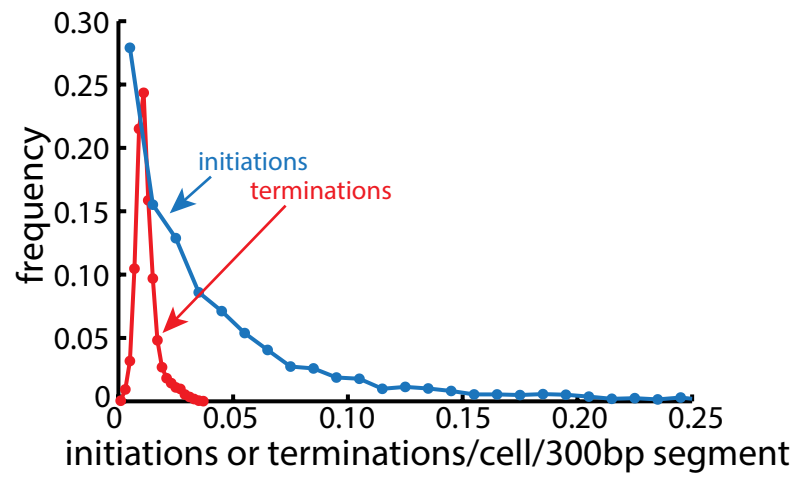


Figure S5

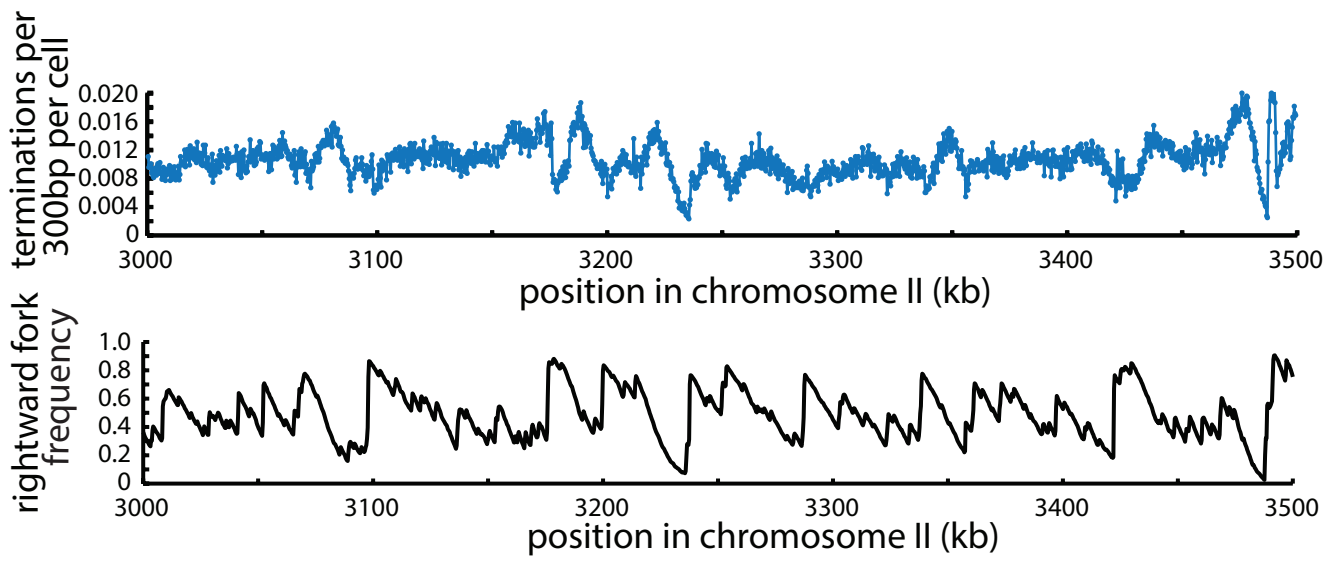


Figure S6

